

# Simultaneous strain and temperature measurement using an integrated fibre Bragg grating/extrinsic Fabry-Perot sensor

T. Liu, G. F. Fernando\*, L. Zhang<sup>a</sup>, I. Bennion<sup>a</sup>, Y. Rao<sup>b</sup>, and D. A. Jackson<sup>b</sup>

Department of Materials Engineering, Brunel University, Uxbridge, Middlesex UB8 3PH, UK.

<sup>a</sup>Department of Electrical Engineering, Aston University, Birmingham B4 7ET, UK.

<sup>b</sup>Physics Department, University of Kent at Canterbury, Canterbury, Kent CT2 7NR, UK

\* To whom correspondence should be addressed.

## ABSTRACT

This paper reports on a novel optical fibre sensor configuration for conducting simultaneous strain and temperature measurements. The sensor consisted of an optical fibre-based extrinsic Fabry-Perot interferometer (EFPI) with an integrated fibre Bragg grating (FBG). The FBG was located within a glass capillary which housed the EFPI sensor and was thus in a strain-free condition. The FBG is primarily sensitive to temperature, whilst the EFPI was sensitive to both strain and temperature. The integrated FBG/EFPI sensor was embedded in a carbon fibre reinforced composite and evaluated. The standard deviation of strain measurement was  $36 \mu\epsilon$  in the range 0 to  $1200 \mu\epsilon$ , and the temperature measurement had a standard deviation of  $3.5^\circ\text{C}$  in the range  $30^\circ$  to  $70^\circ\text{C}$ . The thermal expansion of the cross-ply composite was investigated and was found approximately  $4.05 \times 10^{-6}/^\circ\text{C}$ .

## 1. INTRODUCTION

Fibre optic strain sensors have well-known desirable properties which make them attractive for many applications<sup>1</sup>. Two classes, the fibre Bragg grating (FBG)<sup>2</sup> and the Fabry-Perot (FP) interferometer<sup>3</sup>, show particular promise. One factor limiting their applicability is their cross-sensitivity to transverse strains and temperature. The following techniques have been demonstrated for measuring strain and temperature simultaneously: dual-wavelength FBGs<sup>4,5</sup> FBGs with different cladding diameters<sup>6</sup>, combinations of FBG and polarisation rocking filters<sup>7</sup> or long period gratings<sup>8</sup>; polarisation interferometry<sup>9</sup>; an in-line FP etalon (ILFPE) and an intrinsic FP type interferometer<sup>10</sup> and the use of the mean and the differential group delay in a birefringent optical fibre<sup>11</sup>.

In an earlier paper we used a combination of an FBG and a temperature-insensitive extrinsic FP interferometer (EFPI) to measure strain and temperature in a carbon fibre and epoxy composite<sup>12</sup>. We now report on an improved EFPI sensor design which accommodates an FBG in a strain-free condition. Because of the uncorrelated response of the sensing elements to strain and temperature, this sensor design offers a significant improvement for de-coupling strain from

temperature. Results of in-situ strain and temperature measurements using the embedded FBG/EFPI sensor in carbon fibre reinforced composite are presented. The EFPI sensor was also used to measure the thermal expansion of the composite.

## 2. PRINCIPLE OF SENSOR OPERATION

With reference to Figure 1, the sensor consists of a single mode lead-in/lead-out optical fibre and a multimode fibre reflector. A 5 mm long FBG with a peak wavelength of 851.7 nm was written on the single mode fibre and housed in a 20 mm long quartz capillary (128/300  $\mu\text{m}$  in diameter). Both the single mode and the multimode fibres were fusion spliced onto the capillary. This sensor design essentially consists of an FBG temperature sensor in a strain-free condition which was integrated within an extrinsic Fabry-Perot strain sensor.

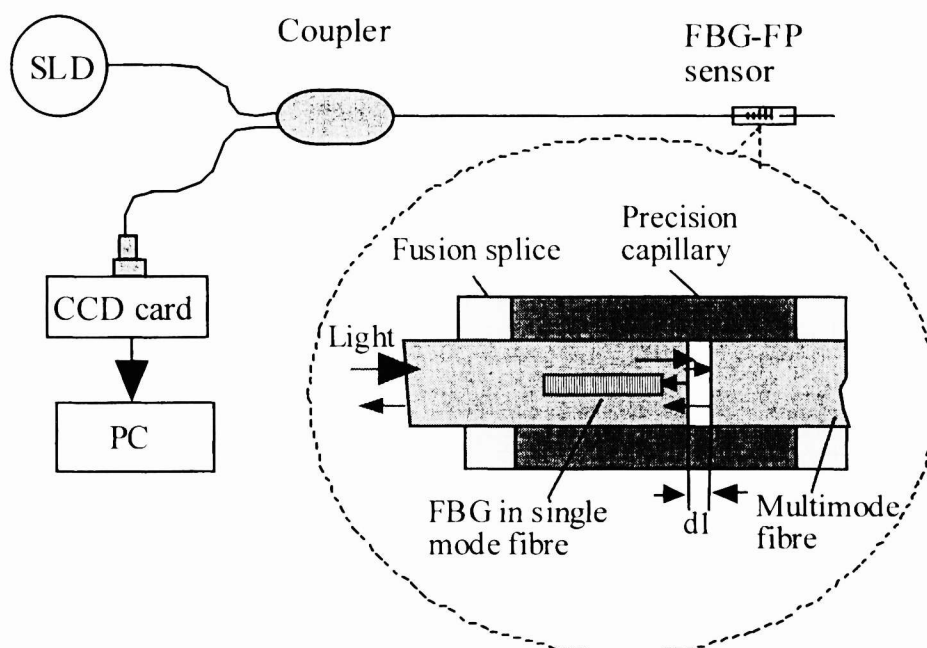


Figure 1 Schematic of the fibre optic strain and temperature sensor system consisting of an integrated FBG and EFPI sensor.

A superluminescent diode (SLD) (Hamamatsu L3302) was used to illuminate the sensors via a single mode coupler. Here a narrow band of the optical power was reflected from the FBG, and the transmitted light was used to illuminate the EFPI sensor. The reflected light from both sensors was detected using a CCD spectrometer (Ocean Optics S1000). The FBG had a very narrow bandwidth with a high reflectivity, whereas the EFPI, being a low finesse interferometer, reflected only a fraction of the total optical power. Hence demultiplexing the FBG and the EFPI sensor was readily achievable.

The reflection spectrum of the EFPI sensor is modulated by its cavity length ( $d$ ). Hence  $d$  can be measured via the free spectral range. When the sensor is embedded in or surface mounted onto the composites, the cavity length can be influenced by the orientation of the sensor in relation to the loading axis, the nature of bonding, the thermal coefficient of the composite and the adhesive, as well as the axial strain. In general the EFPI cavity length can be described by:

$$d = k_{11}\varepsilon + k_{12}\Delta T + d_o \quad (1)$$

where  $\varepsilon$  and  $\Delta T$  represent strain and the change of temperature respectively and  $d_o$  is the cavity length of the EFPI sensor at room temperature in a strain-free condition.  $k_{11}$  has the value of the gauge length ( $L$ ), which is the distance between two fusion splicing points in the EFPI sensor.  $k_{12}$  is determined by the thermal expansion coefficients of the optical fibre ( $\alpha_f$ ), the quartz capillary tube ( $\alpha_q$ ) and the composite ( $\alpha_c$ ) and the sensor gauge length. When the sensor is embedded in a composite,  $k_{12} = L(\alpha_c - \alpha_f)$  and  $k_{12} = L(\alpha_q - \alpha_f)$  when the sensor is placed in air.

The FBG was made from a standard 820 nm single mode optical fibre which was photosensitised by hydrogen loading before UV exposure. The nominal Bragg grating wavelength was 851.7 nm with a 3 dB bandwidth of 0.2 nm and a reflectivity of approximately 40%. The Bragg wavelength shift due to strain and temperature can be described in a general form by:

$$\lambda = k_{21}\varepsilon + k_{22}\Delta T + \lambda_o \quad (2)$$

where  $k_{21}$  and  $k_{22}$  are the effective coefficients for strain and temperature respectively,  $\lambda_o$  is the wavelength under strain free condition at room temperature and  $\Delta T$  is the temperature change relative to room temperature. On combining equations 1 and 2, the following relationship is obtained:

$$\begin{bmatrix} d - d_o \\ \lambda - \lambda_o \end{bmatrix} = \begin{bmatrix} k_{11} & k_{12} \\ k_{21} & k_{22} \end{bmatrix} \begin{bmatrix} \varepsilon \\ \Delta T \end{bmatrix} = K \begin{bmatrix} \varepsilon \\ \Delta T \end{bmatrix} \quad (3)$$

The unknown vector,  $(\varepsilon, \Delta T)^T$ , can be determined by:

$$\begin{bmatrix} \varepsilon \\ \Delta T \end{bmatrix} = K^{-1} \begin{bmatrix} d - d_o \\ \lambda - \lambda_o \end{bmatrix} = \begin{bmatrix} P_{11} & P_{12} \\ P_{21} & P_{22} \end{bmatrix} \begin{bmatrix} d - d_o \\ \lambda - \lambda_o \end{bmatrix} = P \begin{bmatrix} d - d_o \\ \lambda - \lambda_o \end{bmatrix} \quad (4)$$

where  $K$  and  $P$  are matrices which relate the strain and temperature to the EFPI cavity length and the FBG wavelength. In principle, once the components of  $K$  are determined, the strain and temperature can be deduced from the FBG wavelength and the change in the EFPI cavity length. However, the coefficients will be affected by test conditions, for example, the

relative orientation between loading direction and the optical fibre sensor. Therefore, it is generally not appropriate to derive strain and temperature from the  $K$  matrix. Instead they can be inferred by estimating the  $P$  matrix from a population of calibration tests. In this work, the components in the  $P$  matrix were estimated by applying a partial least squares calibration method<sup>13</sup> or the PLS2 algorithm to a population of tests across a range of temperatures and applied strains.

### 3. EXPERIMENTAL

#### 3.1. Thermal response in air

After the sensor was fabricated, the EFPI cavity length was measured. The response of the sensor to temperature in air was then characterised before embedding the sensor in the composite. The sensor was conditioned in an environmental chamber where the temperature was controlled within  $\pm 1^\circ\text{C}$ . The temperature was increased from 20 to  $130^\circ\text{C}$  in steps of  $10^\circ\text{C}$  and was allowed to stabilise for 15 minutes after each increment before measurements were made.

#### 3.2. Sensor embedment

The sensor was embedded between the 4th and 5th ply of a 16-ply carbon fibre reinforced prepreg specimen with a ply lay-up sequence of  $(0, 90_2, 0_2, 90, 0, 90)_s$ . The laminated prepreps were cured according to the manufacturer's recommended cure schedule. The cured composite specimen was end-tabbed to protect it during mechanical loading. The cavity length of the EFPI sensor was measured before and after embedment, hence the residual strain was determined.

#### 3.3. Tensile testing at specified temperatures

An Instron model 1195 tensile testing machine equipped with a temperature controlled environmental chamber was used for these trials. The temperature in the chamber was held at 30, 40, 50, 60 or  $70^\circ\text{C}$ . At each temperature the specimen was loaded from the stress-free state up to 64 MPa in 8 MPa increments. This test was repeated a number of times to assess the reproducibility of the data. The responses of the FBG and the EFPI were evaluated to verify that the FBG was in a strain free condition. A K-type thermocouple was used to measure the temperature within the environmental chamber and it also served as a reference source for the temperature. A surface mounted foil strain gauge (gauge factor of 2.07) was used as the reference source for the applied strain. These data were also used to produce plots of EFPI temperature response at various constant applied stresses. The strain changes observed by the EFPI were assumed to be due to the thermal expansion of the composite only, thus the coefficient of thermal expansion of the composite was evaluated.

## 4. RESULTS AND DISCUSSIONS

The thermal response of the sensor in air is shown in Figures 2 and 3. The analysis of the results indicated that the FBG sensor had a wavelength/temperature coefficient of  $5.6 \pm 0.2 \text{ pm}/^\circ\text{C}$ . The mean measured EFPI cavity length was  $45.5 \mu\text{m}$ , with a standard deviation of less than  $0.15 \mu\text{m}$ . As can be seen from Figure 3, the EFPI sensor prior to embedment had negligible response to temperature.

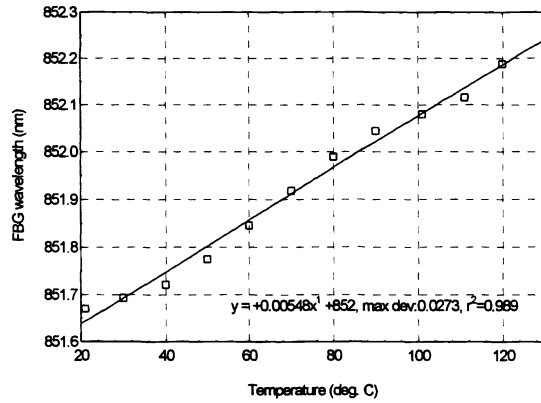


Figure 2 The FBG response vs. temperature in air.

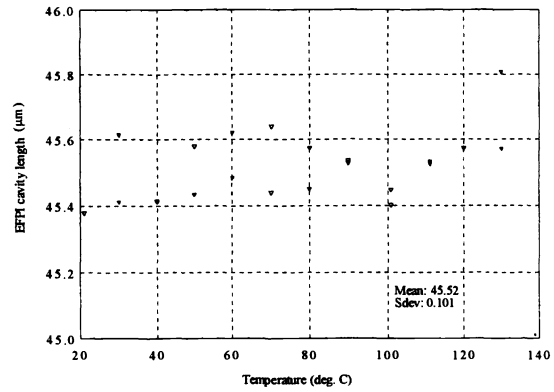


Figure 3 The EFPI cavity lengths vs. temperature in air.

The response of the FBG and the EFPI sensors to strain when tested at room temperature are shown in Figures 4 and 5 respectively. The change in the FBG wavelength did not correlate with tensile strain (the standard deviation of the FBG wavelength was less than 13 pm for a strain range from 0 to 1200  $\mu\epsilon$ ), which suggested that the FBG was in a strain-free condition.

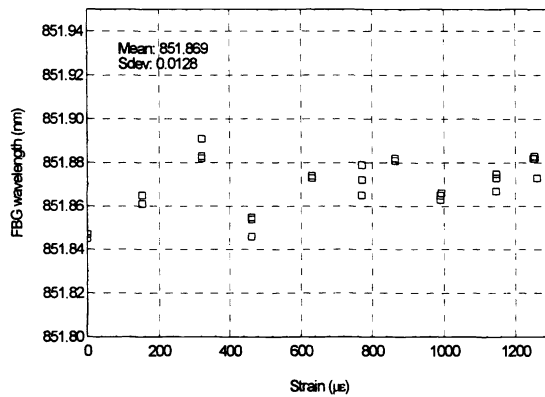


Figure 4 The FBG response to tensile strain.

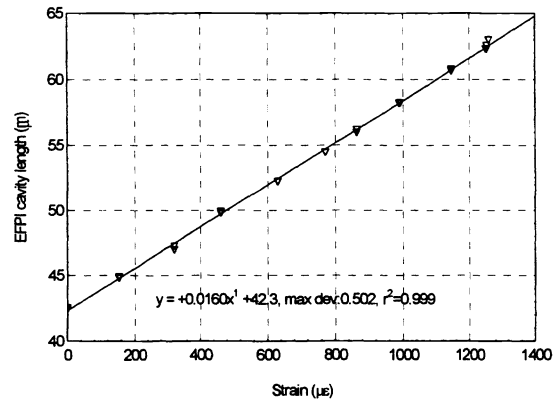


Figure 5 The embedded EFPI response to tensile strain.

The effective gauge length of the EFPI sensor was found from the calibration data in Figure 5 to be 16.3 mm. The EFPI cavity lengths at room temperature, before and after embedment, were 45.5  $\mu\text{m}$  and 42.5  $\mu\text{m}$  respectively. This reduction, of -185  $\mu\epsilon$ , was attributed to residual fabrication strain.

Typical responses of the embedded sensor to applied strain and temperature are shown in Figure 6. The temperature change caused shifts in the FBG peak wavelength, and the applied strain caused a change in the period of the

interference fringes. These reflection spectra were subjected to a normalisation procedure with respect to the emission spectrum of the light source. This in effect enhanced the visibility of the interference fringes.

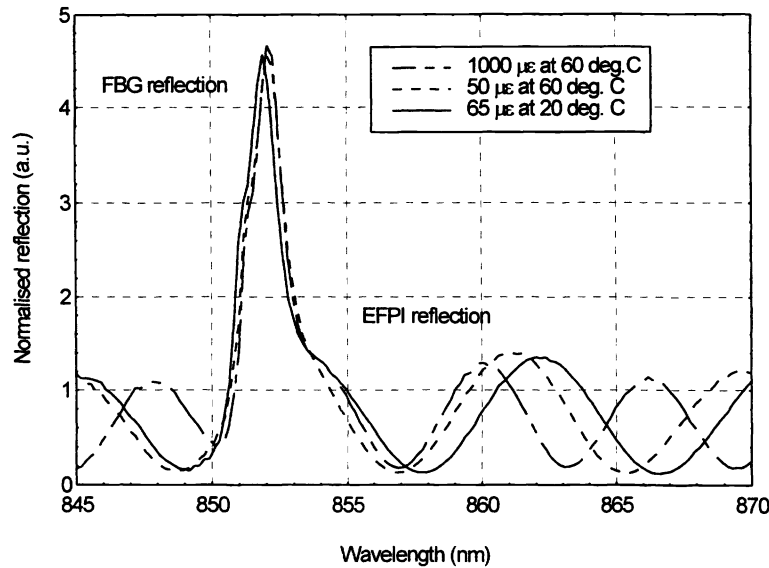


Figure 6 The individual responses of the EFPI and FBG sensors to strain and temperature.

Ninety sets of test data were randomly selected from the temperature range of 30 to 70°C and strain range of 0-1200 µε. A PLS2 partial least squares algorithm with random cross-validation was used to characterise the relative response of the sensors. The conversion matrix for  $P$  was obtained as follows:

$$\begin{pmatrix} \varepsilon \\ \Delta T \end{pmatrix} = P \begin{pmatrix} d - d_o \\ \lambda - \lambda_b \end{pmatrix} = \begin{pmatrix} 63.22 & -139.37 \\ 0.145 & 163.28 \end{pmatrix} \begin{pmatrix} d - 42.5 \\ \lambda - 851.75 \end{pmatrix} \quad (5)$$

Figures 7 and 8 illustrate the observed relationships between the optically measured strain and temperature when compared with the reference data from the thermocouple and strain gauge respectively. The correlation between the measured strain and the reference (strain gauge) data was 99.6%. The corresponding standard deviation was 36 µε for a mean strain of 605 µε. The temperature measurements had a correlation of 98.7% with the reference (thermocouple) data along with a standard deviation of 3.5°C for a mean temperature of 34.5°C.

With reference to equation 5, the EFPI gauge length and the FBG thermal coefficient deduced from  $P_{11}$  and  $P_{22}$  were 15.8 mm and 6.12 pm/°C, respectively. Whereas the pre-calibrated EFPI gauge length at room temperature was 16.3 mm, and the coefficient of thermal expansion for the FBG prior to embedment was 5.6 +/-0.2 pm/°C.

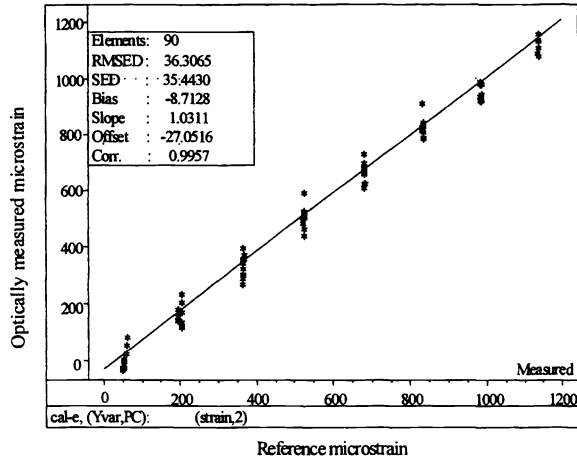


Figure 7 Optically measured strain vs reference data from a surface-mounted strain gauge.

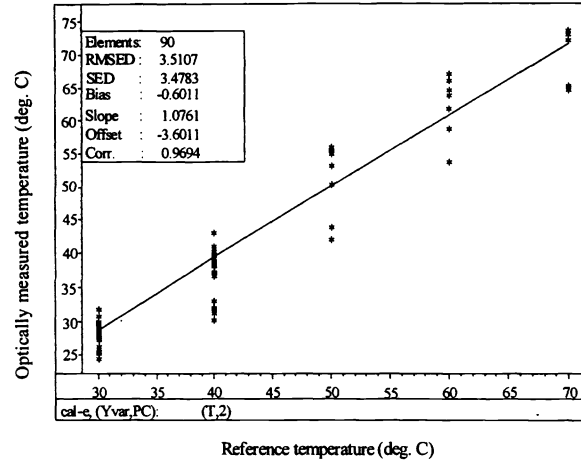


Figure 8 Optically measured temperature vs data from a thermocouple.

The embedded EFPI sensor is immune to transverse strain, thus it is suitable for localised thermal apparent strain measurements when the specimen is under a constant mechanical load. The sensor responses to temperature under constant stresses of 0, 8 and 16 MPa are shown in Figure 9. At each load the thermal apparent strain of the EFPI sensor was approximately  $3.5 \mu\epsilon/^\circ\text{C}$ . Taking the thermal expansion coefficient of the fibre to be that of quartz,  $0.55 \mu\epsilon/^\circ\text{C}$ , the thermal expansion of the composite is  $\approx 4.05 \mu\epsilon/^\circ\text{C}$ .

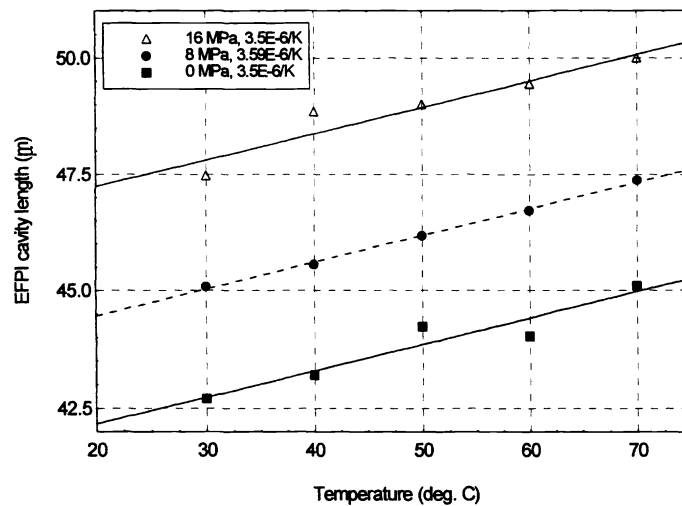


Figure 9 Thermal apparent strain of  $3.5 \mu\epsilon/\text{K}$ , observed under different applied tensile loads.

## 5. CONCLUSIONS

The work presented in this paper demonstrates the following:

- i) the feasibility of including an FBG, in a strain-free condition, within the housing of an EFPI sensor, and of embedding the device in a carbon fibre-epoxy composite;
- ii) that the FBG and EFPI sensors may be interrogated simultaneously for measuring strain and temperature, and
- iii) the combined sensor may be used to find the coefficient of thermal expansion of the host composite.

## 6. REFERENCES

- 1 R. M. Measures, "Fibre optic strain sensing" in *Fibre Optic Smart Structures*, Eric Udd ed. (John Wiley & Sons, Inc. New York ISBN: 0471-554480), 1995.
- 2 H. D. Simonsen, R. Paetsch and J. R. Dunphy, "Fibre Bragg grating sensor demonstration in a glass-fibre reinforced polyester composite", *Proc. 1st Europ. Conf. on Smart Struct. and Mater.*, (Glasgow, UK), pp. 73-76, 1992.
- 3 E. J. Friebele, M. A. Putnam, A. D. Kersey, A. S. Greenblatt, G. P. Ruthven, M. H. Kim and K. S. Gottschalck, "Ultra-high sensitivity strain sensing using fibre cavity etalon", *SPIE 3042*, pp. 100-10, 1997.
- 4 M. G. Xu, J-L, Archambault, L. Reekie, and J. P. Dakin, "Discrimination between strain and temperature effects using dual-wavelength fibre grating sensors", *Electr. Letts 30*, pp. 1085-1087, 1994.
- 5 G. P. Brady, K. Kalli, D. J. Webb, D. A. Jackson, L. Zhang and I. Bennion, "Recent developments in optical fibre Bragg gratings", *SPIE 2839*, pp. 8-19, 1994.
- 6 S. M. James, M. L. Dockney and R. P. Tatam, *Proc. OFS-11* (Sapporo, Japan) Postdeadline Papers Fr3-3 (1996).
- 7 S. E. Kanellopoulos, V. A. Handerek, and A. J. Rogers, "Simultaneous strain and temperature sensing with photogenerated in-fibre gratings", *Opt. Letts 20* (3), pp. 333-335, 1995.
- 8 V. Bhatia, T. D'Alberto, N. Zabaronic and R. O. Claus, "Temperature in-sensitive long-period gratings for strain and refractive index sensing", *Proc. SPIE 3042 Smart Sensing, Processing, and Instrumentation* (San Diego, CA USA 1997) pp. 194-202, 1997.
- 9 F. Farahi, D. J. Webb, J. D. C. Jones, and D. A. Jackson, "Simultaneous measurement of temperature and strain: cross-sensitivity considerations", *J. Lightw. Techn. 8*, pp. 138-142, 1990.
- 10 H. Singh, and J. Sirkis, "Simultaneous measurement of strain and temperature using optical fibre sensors: two novel configurations", pp. 108-111, *Conf. Proc. OFS-11*, Japan, May, 1996.
- 11 D. G. Luke, R. McBride, P. Lloyd, J. G. Burnett, A. H. Greenaway and J. D. C. Jones, "Strain and temperature measurements in composite-embedded highly-birefringent optical fibre using mean and differential group delay", *Proc. 11th Int. Conf. Optical Fibre Sensors* (Sapporo, Japan), pp. 200-203, 1996.
- 12 T. Liu, G. Fernando, Y. Rao, D. A. Jackson, L. Zhang and I. Bennion, "Simultaneous strain and temperature measurements in composite using a multiplexed fibre Bragg grating sensor and an extrinsic Fabry-Perot sensor", *SPIE 3042* 203-212, 1997.
- 13 H. Martens and T. Naes, *Multivariate calibration*, Wiley: Chichester, 1989.